Extensive air showers from ultrahigh energy gluinos

V. Berezinsky

INFN, Lab. Naz. del Gran Sasso, I-67010 Assergi (AQ), Italy

M. Kachelrieß

TH Division, CERN, CH-1211 Geneva 23, Switzerland

S. Ostapchenko

Forschungszentrum Karlsruhe, Institut für Kernphysik, D-76021 Karlsruhe, Germany
and Moscow State University, Institute of Nuclear Physics, 199899 Moscow, Russia

We study the proposal that the cosmic ray primaries above the Greisen-Zatsepin-Kuzmin cutoff are gluino-containing hadrons ($\tilde{g}$ hadrons). We describe the interaction of $\tilde{g}$ hadrons with nucleons in the framework of the Gribov-Regge approach using a modified version of the hadronic interaction model QGSJET for the generations of extensive air showers (EAS's). There are two mass windows marginally allowed for gluinos: $m_{\tilde{g}} \lesssim 3$ GeV and $25 \lesssim m_{\tilde{g}} \lesssim 35$ GeV. Gluino-containing hadrons corresponding to the second window produce EAS's very different from the observed ones. Light $\tilde{g}$ hadrons corresponding to the first gluino window produce EAS's similar to those initiated by protons, and only future detectors will be able to marginally distinguish them. We propose a beam-dump accelerator experiment to search for $\tilde{g}$ hadrons in this mass window. We emphasize the importance of this experiment: it can discover (or exclude) the light gluino and its role as a cosmic ray primary at ultrahigh energies.

PACS number(s): 98.70.Sa, 14.80.−j

I. INTRODUCTION

For a long time light gluinos have attracted attention as possible carriers of the very high energy signal in the universe. In the 1980s, they were studied as a possible primary particle from Cyg X-3 [1,2] and now as a primary particle of the observed ultrahigh energy cosmic rays (UHECR's) [3,4].

The observations of UHECR's with energies above 10^{20} eV impose a serious problem (see [5] for recent reviews). The data show the presence of a new, nearly isotropic component in the UHECR flux above the energy $E \sim 10^{19}$ eV [5]. Since the arrival directions of the UHECR's show no correlation with the galactic plane and the galactic magnetic field cannot isotropize particles of such energies, this component is thought to be extragalactic. The clustering of events (doublets and triplets) favors extragalactic sources with large space density [6]. On the other hand, the signature of extragalactic protons, the Greisen-Zatsepin-Kuzmin (GZK) cutoff [7] at $E \simeq 6 \times 10^{19}$ eV, is not found. The other natural UHE primaries, nuclei and photons, suffer a similar cutoff [8,9] or are absorbed at cosmologically short distances [10], respectively. Meanwhile, four different UHECR experiments [5] do not show the presence of such a cutoff. The two highest energy events were detected by the AGASA [11] and Fly's Eye [12] experiments, at an energy of 2×10^{20} eV and 3×10^{20} eV, respectively. The total number of events with an energy higher than 1×10^{20} eV is about 30, 17 of which were detected by AGASA [13]. The accuracy of the energy determination is estimated to be better than 20–30 %. The energies of the two highest energy events [11] and [12] were determined very reliably. To resolve this puzzle, it seems that new ideas in astrophysics or particle physics are required.

The prediction of the GZK cutoff is robust in all models assuming a homogeneous distribution of extragalactic sources with conservatively steep generation spectra; the cutoff is more pronounced if the maximal energy of acceleration is not too high, $E_{\max} \lesssim 1 \times 10^{21}$ eV. The simplest modifications of these models, which use flat generation spectra with index $\gamma_g = 2.0$–2.1 and unlimited maximal energy [14,15], have a less sharp GZK cutoff and contradict the data only moderately. However, they need large cosmic ray luminosities and high acceleration energies, which is a problem for sources with large space density [16]. A reasonable illustration of this possibility is given by gamma ray burst models, which predict UHECR fluxes two or three orders of magnitude less than observed [17,18] and a spectrum in disagreement with observations outside a narrow energy interval [18]. In contrast, steep generation spectra with $\gamma_g \approx 2.7$ give excellent agreement with observations for an energy range as wide as 1×10^{17}–8×10^{19} eV, but predict a sharp GZK cutoff [18]. The other simple modification, assuming a local overdensity of sources, also does not work very efficiently [15,18]. However, astrophysical solutions cannot be considered as excluded at present.

The proposals involving particle physics include UHE particles from superheavy dark matter [19] and topological defects [20], the resonant interaction of UHE neutrinos with dark matter neutrinos [21], strongly interacting neutrinos [22], new particles as UHE primaries [3,4,23], and such a radical possibility as Lorentz invariance violation [24]. (For more references see also the reviews cited in [5].)

In this paper, we shall consider a gluino-containing hadron ($\tilde{g}$ hadron) as a carrier of the cosmic UHE signal, being inspired by the correlation between active galactic nuclei

(AGN) and arrival directions of UHE particles suggested by the analyses in Refs. [4,25,26]. The strongest correlation was found between UHE primaries and BL Lacs in Ref. [26]. Being a rare subpopulation of AGN's, the lacertids are distributed uniformly in the universe at large distances from each other and thus from our galaxy. Therefore UHECR's generated by them must have the GZK cutoff. Its absence implies that the primaries are not absorbed on the cosmic microwave background radiation (CMBR). The correlation of UHECR arrival directions with low-space-density, homogeneously distributed extragalactic sources favors a neutral signal carrier. In fact, six of nine UHE candidates for correlation (see Table 1 from [26]) arrive from the direction of BL Lacs with redshifts $z > 0.138$, i.e., at distances $r > 640$ Mpc.

Hence the correlation with BL Lacs, if confirmed, most probably implies a neutral signal carrier not absorbed on the CMBR. A light gluino is a suitable candidate for such a primary: it can be efficiently produced in pp interactions in astrophysical sources, it is not strongly absorbed by CMBR (see below), and it produces EAS's in the atmosphere very similar to those observed. Heavy gluinos are naturally produced in decays of superheavy particles [27], but initiate EAS's clearly distinguishable from those of protons.

We shall study here the interaction of both light and heavy gluinos with nucleons at UHE. In most interesting applications gluinos must be light (see below). To be a suitable primary of UHECR's, the $\tilde{g}$ hadron should satisfy three conditions.

(1) The longitudinal shower profile of the Fly's Eye highest-energy event with $E = 3 \times 10^{20}$ eV is well fitted by a proton [28,29], although the Fly's Eye Collaboration does not exclude a photon as a primary [12]. Therefore, $\tilde{g}$ hadrons should essentially mimic proton (or photon) induced air showers.

(2) To shift the GZK cutoff to higher energies, the new hadron should have a mass in excess of the proton mass: the threshold energy for any energy-loss reaction on microwave photons increases with increasing primary mass, while the fraction of energy lost per scattering decreases. Moreover, it is desirable that its cross section for interactions with CMBR photons is smaller than that of the proton. This can be achieved if, e.g., the mass of the first resonance X that can be excited in the reaction $\tilde{g}$ hadron$+ \gamma_{CMBR} \rightarrow X$ is relatively large.

(3) The primary has to be stable or quasistable with lifetime $\tau \gtrsim 10^6$ s $(m/\text{GeV}) (L/\text{Gpc})$ in order to survive its travel from a source (e.g., an AGN) at a distance $L \sim 100–1000$ Mpc from the earth.

In principle gluino-containing hadrons ($\tilde{g}$ hadrons) could satisfy the above requirements. Below we shall briefly review the status of $\tilde{g}$ hadrons as UHECR signal carriers.

To satisfy the third condition, the gluino should be the lightest supersymmetric particle (LSP), or have a very small mass difference from the LSP. It also can be the second lightest supersymmetric particle, if the LSP is the gravitino; in this case the gluino decays gravitationally and its lifetime can be long enough. Theoretically the best motivated candidates for the LSP are the neutralino and gravitino. While in

minimal supergravity models the LSP is the lightest neutralino (in some part of the parameter space it is the sneutrino), in models with gauge-mediated supersymmetry (SUSY) the LSP is normally the gravitino. In Farrar's model [30], the gluino is the LSP because the dimension-three SUSY breaking terms are set to zero. A theoretically more appealing scenario containing a light gluino was developed in Refs. [31,32]. There, the gluino with mass 1–100 GeV was found in a SO(10) model with gauge-mediated SUSY breaking and Higgs-boson–messenger mixing. In this model either the gluino or the gravitino is the LSP. In the latter case, the gluino can decay but has a sufficiently long lifetime to be a viable UHECR primary, $\tau \sim 100$ yr.

In a physical state, the gluino is bound into colorless hadrons. What is the lightest state of gluino-containing hadrons?

In the 1980s (see [2]), it was argued on the basis of QCD sum rules that the *glueballino* $\tilde{g}g$ is the lightest $\tilde{g}$ hadron. The lightest baryonic state, the *gluebarino*, was demonstrated to be the $\bar{g}uud$ hadron [33]. The gluebarino is a long-lived particle because its decay needs violation of either baryon number or R parity [33]. More recently, Farrar proposed [30] the neutral hadron S^0, a $\tilde{g}uds$ bound state, as the lightest $\tilde{g}$ hadron (see also the calculations in the MIT bag model of Ref. [34]).

There is some controversy if a light gluino, with a mass of a few GeV, is allowed. As it stands, the Farrar model [30] is in conflict with searches for glueballino decays [35–37] as well as for decays of other unstable $\tilde{g}$ hadrons [38]. However, these searches were restricted to a narrow band of lifetimes and masses, and their results are not valid in the context of more generic models.

The existence of a light gluino ($m_{\tilde{g}} \lesssim 5$ GeV) can be (dis)proved due to its contribution to the running of α_s and to QCD color coefficients in an essentially model-independent way. The authors of Ref. [39] used the ratio R between the hadronic and $\bar{\mu}\mu$ production cross sections in $e^+ e^-$ annihilation at different energies to constrain the light gluino scenario. They excluded light gluinos with mass $m_{\tilde{g}} = 3(5)$ GeV with 93(91)% C.L, while the mass range $\lesssim 1.5$ GeV remained essentially unconstrained. Combining these results with the determination of QCD color coefficients from the analysis of multijet events in [40], the conclusions of [39] became much stronger: light gluinos with mass $\lesssim 5$ GeV were excluded with at least 99.89% C.L. The analysis of multijet events relied, however, on the use of Monte Carlo simulations whose parameters are tuned to QCD without light gluinos. Moreover, the multijet analysis was based on a tree-level calculation with rather large scale ambiguities. The assessment of these uncertainties is difficult, thus preventing the definite exclusion of a very light gluino by this argument [41,42].

Direct accelerator limits for the gluino as the LSP were discussed recently in Refs. [32,43,44]: The authors of Ref. [43] concluded that the range 3 GeV$\lesssim m_{\tilde{g}} \lesssim$ 130–150 GeV can be excluded at 95% C.L. based on currently available OPAL and Collider Detector at Fermilab (CDF) data. Their results are sensitive to the details of the hadronic interactions

of $\tilde{g}$ hadrons and, for certain choices of the parameters, a window in the intermediate mass region 23 GeV$\lesssim m_{\tilde{g}}$ $\lesssim 50$ GeV remains open. Meanwhile, Ref. [32] noted that these limits could be weakened if squarks are not very heavy and contribute to the jet + missing energy signal, while Ref. [44] confirmed an open window for a gluino with 25 GeV $\lesssim m_{\tilde{g}} \lesssim 35$ GeV.

We also mention here that cosmological constraints do not exclude either light and heavy gluinos of interest [27,45]. The Gustafson experiment [47] also does not exclude $\tilde{g}$ hadrons (see Sec. V).

Until now we have discussed the limits on the gluino mass $m_{\tilde{g}}$. The lightest $\tilde{g}$ hadron with mass $M_{\tilde{g}}$ is heavier than the gluino by the mass of its constituent gluon or quarks, which is expected to be less than 1 GeV.

Light $\tilde{g}$ hadrons with $M_{\tilde{g}} \sim 1.5$ GeV have a spectrum with the GZK cutoff beyond the currently observed energy range (see [27] and Fig. 13 of the present paper). Together with the accelerator limits on gluino masses, this leaves a narrow band of allowed masses for the light $\tilde{g}$ hadrons at $1.5 \lesssim M_{\tilde{g}} \lesssim 4$. But this window is closed if, as argued in [33], the charged gluebarino $\tilde{g}uud$ is lighter than the neutral $\tilde{g}uds$. Indeed, production of charged gluebarinos in the earth's atmosphere by cosmic rays and their accumulation in the ocean results in too high an abundance of "wild hydrogen" in contradiction with observational data. In Refs. [30,34], however, it is argued that the lightest gluebarino is the neutral flavor singlet $\tilde{g}uds$, due to strong quark attraction in this state. But even in this case the restriction [33] might work, if the $\tilde{g}uds$ gluebarino and proton are bound into anomalous deuterium.

In conclusion, a light gluino—although disfavored by various arguments—is not excluded. We study here the interactions of gluinos, being inspired by a possible correlation between AGN's and the arrival directions of UHECR's [4,25] and by the recent suggestion [3,48], that extensive air showers (EAS's) observed at the highest energies could be produced by $\tilde{g}$ hadrons. The authors of Ref. [48] performed a detailed simulation of EAS's induced by $\tilde{g}$ hadrons, using, however, a phenomenological description for the $\tilde{g}$ hadron–nucleon interaction that is not self-consistent. They found that masses as high as 50 GeV are compatible with presently available data. In contrast, it was argued in Ref. [27], using kinematical arguments, that the observed shower characteristics exclude any strongly interacting particle much heavier than a few GeV.

The purpose of the present work is to study EAS's produced by $\tilde{g}$ hadrons and to restrict the mass range in which the $\tilde{g}$ hadron is a viable UHE primary using a self-consistent interaction model. We have used for the simulation of air showers initiated by $\tilde{g}$ hadrons a suitably modified version of the QGSJET model [49,50] which is known to describe proton air showers successfully [49,51]. Specifically, we have considered the glueballino as the $\tilde{g}$ hadron but we expect that our results apply to all $\tilde{g}$ hadrons. We paid special attention

to consistent calculations of glueballino-hadron interaction cross sections and of cascade particle production in the atmosphere. We found that the development of showers initiated by $\tilde{g}$ hadrons with masses above 5 GeV differs substantially from that of proton-initiated showers and is inconsistent with the current experimental data. In the window of masses 1.5–4 GeV, where a $\tilde{g}$ hadron can be allowed, glueballino-induced showers do not contradict the available data. Future observations by the detectors HiRes and Auger can either confirm or exclude $\tilde{g}$ hadrons as the dominant primary, combining the information from shower profiles and the energy spectrum. However, the best way to test this hypothesis is a modified Gustafson experiment (see Sec. V). In the case of the discovery of light $\tilde{g}$ hadrons in such an experiment, we shall reliably know their properties, thus enabling us to calculate the production of these particles in astrophysical sources and their detection in the earth's atmosphere. Their absence will preclude further discussion of this hypothesis.

II. GLUEBALLINO-PROTON (NUCLEUS) INTERACTION

A. QGSJET framework

QGSJET, a Monte Carlo generator of hadron-hadron, hadron-nucleus, and nucleus-nucleus interactions [49,50], was developed in the framework of the Gribov-Regge approach and is based on the quark-gluon string model of the supercritical Pomeron [52]. Hadronic interactions are described as a superposition of elementary rescattering processes between the partonic constituents of the projectile and target nucleons (hadrons), resulting in the production of color neutral strings, which further fragment into secondary hadrons. The key parameters of the model are the intercepts and slopes of the Regge trajectories of the Pomeron and of secondary Reggeons. These parameters govern the formation of different interaction configurations, how the energy-momentum is shared in elementary interactions, and also the string hadronization. The model was generalized to hadron-nucleus and nucleus-nucleus interactions in the framework of the Glauber-Gribov approach [53,54], taking into account low mass diffraction and inelastic screening processes [55]. Hard QCD processes were included into the Gribov-Regge formalism via the concept of a "semihard Pomeron," which is a t-channel iteration of the soft Pomeron and a QCD parton ladder contribution [50,56].

QGSJET describes hadron-hadron interaction amplitudes as a sum of two contributions, namely, soft and semihard rescattering [50]. The soft contributions are of purely nonperturbative nature and correspond to the case of a parton cascade with virtualities smaller than some cutoff Q_0^2. Below this cutoff, perturbative QCD is not applicable and the interaction is described by phenomenological soft Pomeron exchange. The amplitude $f_{ac}^{\mathbb{P}}$ for Pomeron exchange between two hadrons a and c is given by [52]

$$f_{ac}^{\mathbb{P}}(s,b) = \frac{\gamma_a \gamma_c \exp(\Delta y)}{\lambda_{ac}(y)} \exp\left(-\frac{b^2}{4\lambda_{ac}(y)}\right), \quad (1)$$

$$\lambda_{ac}(y) = R_a^2 + R_c^2 + \alpha'_{\mathbb{P}} y, \tag{2}$$

where $y = \ln s$ is the rapidity size of the Pomeron, s is the squared center-of-mass energy for the interaction, b is the impact parameter between the two hadrons, and the parameters $\gamma_{a(c)}$ and $R_{a(c)}^2$ are the vertices and slopes for the Pomeron–hadron $a(c)$ coupling, respectively. Finally, Δ and $\alpha'_{\mathbb{P}}$ are the parameters describing the overcriticality and the slope of the soft Pomeron trajectory.

In contrast to soft rescatterings, semihard ones correspond to the case when at least a part of the parton cascade develops in the region of parton virtualities $q^2 > Q_0^2$ and, therefore, can be described on the basis of QCD techniques. The complete semihard contribution is represented by a QCD parton ladder sandwiched between two soft Pomerons [56]. For the Pomeron, the formulas (1) and (2) can still be used. However, since it is now coupled to a hadron $a(c)$ on one side but to a parton ladder on the other side, the slope $R_{c(a)}^2$ and the coupling $\gamma_{c(a)}$ have to be replaced by the slope R_{lad}^2 and the coupling $V_{\text{lad}}^{\mathbb{P}}$ of the Pomeron-ladder. The latter is parametrized as

$$V_{\text{lad}}^{\mathbb{P}}(y) = r[1 - \exp(-y)]^{\beta_{\mathbb{P}}}, \tag{3}$$

where the parameters r and $\beta_{\mathbb{P}}$ describe the momentum distribution of a parton (sea quark or gluon) in the soft Pomeron. Using $R_{\text{lad}}^2 \simeq 1/Q_0^2 \ll R_{a(b)}^2 + \alpha'_{\mathbb{P}} y$, the slope R_{lad}^2 can be neglected.

To complete the description of soft and semihard contributions, the momentum distribution function $N_a^{\mathbb{P}}$ for soft Pomeron emission by a hadron of type a has to be specified. It is parametrized in the form

$$N_a^{\mathbb{P}}(x_{\mathbb{P}}^{\pm}) \sim (x_{\mathbb{P}}^{\pm})^{\alpha}(1 - x_{\mathbb{P}}^{\pm})^{\beta_a}, \tag{4}$$

where the first factor does not depend on the hadron type and describes the probability of slowing down the hadron constituents to which the Pomeron is connected. In QGSJET, the Pomeron is connected to a (dressed) quark-antiquark pair. Using Regge asymptotics [52], i.e., $\alpha_{q\bar{q}} \simeq 0.5$ as the intercept of the Regge $q\bar{q}$ trajectory for light quarks, it follows that

$$\alpha = 1 - 2\alpha_{q\bar{q}} \simeq 0. \tag{5}$$

Similar, the second factor in Eq. (4) describes the probability of slowing down the "leading" hadron state configuration; the parameter β_a is expressed via the intercept $\alpha_{a\bar{a}}$ of the corresponding Regge trajectory as $\beta_a = -\alpha_{a\bar{a}}$.

The semihard contribution described above corresponds to the case that gluons or sea quarks of the hadron start the interaction at the initial scale Q_0^2. Additionally, valence quarks can interact with $q^2 \geq Q_0^2$. Then the only nonperturbative inputs needed are the valence quark momentum distributions $q_v(x, Q_0^2)$ at the initial scale Q_0^2.

B. Extension for glueballino

The nucleon-glueballino interaction can be treated in the QGSJET model in the same framework as the one for the usual

hadrons [49]. The main difficulty is to connect the unknown physical parameters (coupling $\gamma_{\tilde{G}}$, slope $R_{\tilde{G}}^2$, and momentum distribution $N_{\tilde{G}}^{\mathbb{P}}$) describing the interactions of glueballinos with the corresponding quantities of the usual hadrons. We use simple scaling arguments to derive the glueballino parameters from those of the pion.

(1) The coupling γ_a of a hadron a to the Pomeron depends essentially on its size and, consequently, on its reduced mass M_a. If r_a denotes the radius of the hadron a with the reduced mass M_a, then $\gamma_a \sim r_a^2 \sim M_a^{-2}$, where we have neglected a factor $\alpha_s(M_a^2)$ in the last step. Thus, the Pomeron-glueballino vertex $\gamma_{\tilde{g}}$ can be expressed via the Pomeron-pion vertex γ_{π} as

$$\gamma_{\tilde{G}} = \gamma_{\pi} \left(\frac{M_{\pi}}{M_{\tilde{G}}} \right)^2. \tag{6}$$

For the reduced mass $M_{\tilde{G}}$ of the glueballino, we use

$$M_{\tilde{G}} = \frac{m_{\tilde{g}} m_g}{m_{\tilde{g}} + m_g}, \tag{7}$$

where $m_{\tilde{g}}$ is the mass of the gluino and $m_g \simeq 0.7$ GeV is the constituent mass of the gluon. Similarly, we use for the pion $M_{\pi} = m_q/2$ with $m_q \simeq 0.35$ GeV as quark constituent mass. Note that Eq. (6) does not take into account the different color factors of quarks and gluon/gluinos because we consider an effective Pomeron coupling to the hadron as a whole, not to individual parton constituents.

(2) The slope $R_{\tilde{G}}^2$ for the Pomeron-glueballino coupling is also inverse proportional to $M_{\tilde{G}}^2$. Therefore, $R_{\tilde{G}}^2$ is small compared to R_p^2 and $R_{\mathbb{P}}^2 = \alpha'_{\mathbb{P}} y$ and can be neglected in the formulas (1), (2),

$$\lambda_{\tilde{G}p}(y) \simeq R_p^2 + \alpha'_{\mathbb{P}} y. \tag{8}$$

(3) The momentum distribution for Pomeron emission is again given by Eq. (4), $N_{\tilde{G}}^{\mathbb{P}} \sim (x_{\mathbb{P}}^{\pm})^{\alpha}(1 - x_{\mathbb{P}}^{\pm})^{\beta_{\tilde{G}}}$. Now the "leading" configuration consists of a valence gluon and gluino,

$$\beta_{\tilde{G}} = 1 + \beta_{\tilde{g}} + \beta_g. \tag{9}$$

Assuming that a valence gluon behaves similarly to a valence $q\bar{q}$ pair in the low-x limit gives $\beta_g \simeq 1 - 2\alpha_{q\bar{q}} \simeq 0$. The remaining unknown parameter $\beta_{\tilde{g}}$ can be found from the momentum distribution between the valence constituents of the glueballino. Using as ansatz for the momentum distribution $\rho_{\tilde{g}}^{\tilde{G}}$ of the gluino

$$\rho_{\tilde{g}}^{\tilde{G}}(x_{\tilde{g}}) \sim x_{\tilde{g}}^{\beta_{\tilde{g}}}(1 - x_{\tilde{g}})^{\beta_g} \tag{10}$$

and assuming that the energy is shared according to the constituent masses of the valence partons, we obtain for the average momentum fraction carried by the gluino

$$\langle x_{\tilde{g}}\rangle = \frac{m_{\tilde{g}}}{m_g + m_{\tilde{g}}} = \frac{\beta_{\tilde{g}} + 1}{\beta_g + \beta_{\tilde{g}} + 2}. \tag{11}$$

This results in

$$\beta_{\tilde{g}} = \frac{m_{\tilde{g}}}{m_g}(\beta_g + 1) - 1 \simeq \frac{m_{\tilde{g}}}{m_g} - 1. \tag{12}$$

Having fixed the free parameters describing the Pomeron-glueballino interactions using essentially only one simple, physically well-motivated scaling argument, the soft and semihard contributions are determined. These two contributions to the total nucleon-glueballino interaction are referred to below as the contribution due to the *soft coupling*, because they are both caused by soft Pomeron emission of the glueballino.

To complete the formalism, we need to define the momentum distribution of the valence gluon or gluino inside the glueballino probed at the initial scale Q_0^2, when they are involved in hard interactions. We shall refer to this contribution below as the the contribution due to the *direct coupling*. Parton emission by a gluino in the s channel is strongly suppressed kinematically in the nonperturbative region $q^2 < Q_0^2$ by its mass: the virtuality q^2 of the process $\tilde{g} \rightarrow g + \tilde{g}$ is determined by the off-shellness $|q_{\tilde{g}}^2 - M_{\tilde{g}}^2|$ of the t channel gluino produced,

$$q_{\tilde{g} \rightarrow g}^2 = |q_{\tilde{g}}^2 - M_{\tilde{g}}^2| = \frac{p_\perp^2}{1-z} + M_{\tilde{g}}^2(1-z). \tag{13}$$

Here $p_\perp$ and z are the transverse momentum and the light cone momentum fraction for the t-channel gluino. Therefore, the gluino momentum distribution at the scale Q_0^2 essentially remains in the form (10),

$$\tilde{g}_v(x_{\tilde{g}}, Q_0^2) = \rho_g^{\tilde{G}}(x_{\tilde{g}}). \tag{14}$$

TABLE I. Total cross section σ_{tot}, inelastic cross section σ_{in}, cross section due to soft coupling $\sigma_{\text{tot}}^{\text{s coupl}}$, cross section due to direct coupling $\sigma_{\text{tot}}^{\text{d coupl}}$, cross section without hard interactions σ_{AFK} and inelasticity coeffiecent K_{inel} for glueballino-nucleon scattering. The data are given for four values of the glueballino mass $M_{\tilde{G}}$ from 2 GeV to 50 GeV at glueballino energy $E_{\text{lab}} = 100$ GeV. As references, the total and inelastic cross sections of the pion are also given. All cross sections are in mb.

		$M_{\tilde{G}}$			
	π	2 GeV	5 GeV	10 GeV	50 GeV
σ_{tot}	24.4	3.9	2.9	2.4	2.2
σ_{in}	20.9	3.8	2.8	2.4	2.1
$\sigma_{\text{tot}}^{\text{s coupl}}$		3.8	2.7	2.4	2.2
$\sigma_{\text{tot}}^{\text{d coupl}}$		0.14	0.15	0.013	0
σ_{AFK}		3.8	2.7	2.4	2.2
K_{inel}		0.25	0.15	0.074	0.0054

TABLE II. The same as Table I for $E_{\text{lab}} = 10^{12}$ GeV.

		$M_{\tilde{G}}$			
	π	2 GeV	5 GeV	10 GeV	50 GeV
σ_{tot}	152	103	94.9	91.3	88.0
σ_{in}	112	71.3	65.9	63.4	60.2
$\sigma_{\text{tot}}^{\text{s coupl}}$		85.5	69.4	61.8	50.8
$\sigma_{\text{tot}}^{\text{d coupl}}$		72.1	72.4	72.3	74.4
σ_{AKF}	92.2	18.2	13.3	11.8	10.6
K_{inel}		0.26	0.14	0.082	0.018

By contrast, the momentum distribution of the valence gluon differs from $\rho_g^{\tilde{G}}(1-x_g)$ in Eq. (10) because of the emission of sea quarks and gluons (due to the soft coupling defined above),

$$g_v(x_g, Q_0^2) \sim x_g^{\beta_g}(1-x_g)^{\beta_{\tilde{g}} + \delta}. \tag{15}$$

The parameter δ is fixed by the momentum conservation constraint for the complete (valence and sea) parton momentum distributions at the initial scale Q_0^2. This completes the formulation of the initial conditions for the perturbative evolution.

The treatment of the perturbative part of the interaction is performed to leading-logarithmic accuracy; the corresponding techniques are described in Ref. [49]. All emitted (s-channel) partons undergo timelike cascading according to the standard algorithm [57], with soft gluon coherence taken into account. At the final stage, soft strings are assumed to be formed between on-shell partons according to their color connection pattern. The final gluino is assumed to pick up a gluon-gluon singlet pair from the vacuum. After a color rearrangement similar to the one in J/ψ production, a glueballino is formed. String hadronization completes the procedure for glueballino-hadron interaction. The extension of the model to glueballino-nucleus collisions is based on the standard Glauber-Gribov approach and does not differ from the usual hadron-nucleus case [55].

C. Numerical results

The model developed in the last subsection allows both calculation of the cross sections for glueballino-nucleon interactions and consistent treatment of particle production in these reactions. Some quantities characterizing the glueballino-nucleon interactions are given in Table I for $E_{\text{lab}} = 100$ GeV and in Table II for $E_{\text{lab}} = 10^{12}$ GeV. We present both total and inelastic cross sections as well as the partial contributions arising due to the soft ($\sigma_{\text{tot}}^{\text{s coupl}}$) and direct ($\sigma_{\text{tot}}^{\text{d coupl}}$) coupling of the glueballino.[1] At low energies, the soft coupling strongly dominates the $\tilde{G}$-proton interaction for all $M_{\tilde{G}}$, being governed by nonperturbative soft interactions, while the direct coupling can be neglected. At

---

[1] Note that the total cross section is smaller than the sum of the partial contributions $\sigma_{\text{tot}}^{\text{s coupl}}$ and $\sigma_{\text{tot}}^{\text{d coupl}}$, because it contains contributions from multiple rescatterings of both types.

high energies, this picture changes considerably. The soft coupling becomes more and more suppressed for large $M_{\widetilde{G}}$. By contrast, the direct contribution, which is purely perturbative on the glueballino side, is nearly independent of $M_{\widetilde{G}}$. This important difference from the usual hadron case is due to the very asymmetric energy partition between the parton constituents of the glueballino. For large $M_{\widetilde{g}}$, the valence gluino carries almost the whole initial energy of the particle (88% for $M_{\widetilde{g}}=5$ GeV and 99% for $M_{\widetilde{g}}=50$ GeV)—Eqs. (10), (11), and (14)—thus leaving just a small part of it to other partons, to which Pomerons are connected. Therefore, the glueballino behaves in the limit of large $M_{\widetilde{G}}$ essentially as a perturbative object, as one expects from kinematical considerations [27]. Finally, the last row of the tables shows the inelasticity coefficient K_{inel} as another important quantity which distinguishes proton-proton and $\widetilde{G}$-proton interactions. Although at energies of interest for UHECR's the total cross section for $\widetilde{G}$-proton interactions is rather large, a heavy glueballino behaves like a penetrating particle in the atmosphere, losing only a small part of its energy in one interaction. This conclusion was already reached in Ref. [27] from semiqualitative considerations. The reason for this effect is twofold. On one hand, as discussed above, gluinos of larger masses carry a larger fraction of the initial particle energy, leaving a smaller part of it for the sea constituents [(anti)quarks and gluons] and thus reducing the average number of multiple interactions in $\widetilde{G}$-proton (nucleus) collisions. On the other hand, the relative weight of the "direct hard" process increases for heavier gluinos, where the valence gluino loses typically only a small part of its energy, as a large longitudinal momentum transfer is strongly suppressed in that case by the process virtuality $q^2_{\widetilde{g}\rightarrow g}$,

$$q^2_{\widetilde{g}\rightarrow g}=\frac{p^2_\perp}{1-z}+\frac{z^2 M^2_{\widetilde{g}}}{1-z}, \tag{16}$$

with $p_\perp$ and z being the transverse momentum and the light cone momentum fraction for the emitted t-channel gluon of the initial valence gluino, which mediates the gluino hard interaction with the target proton (nucleus).

We show also in Figs. 1 and 2 the total and inelastic cross sections as functions of the interaction energy E_{lab} for glueballino masses $M_{\widetilde{g}}=2,5$, and 50 GeV. The fast increase of the direct contribution with E_{lab} produces an interesting effect: the total interaction cross section for the largest glueballino mass considered, $M_{\widetilde{G}}=50$ GeV, which is dominated by the direct contribution, overshoots the ones for smaller glueballino masses in the energy range 10^4–10^9 GeV.

III. EXTENSIVE AIR SHOWERS

In this section, we present some results of our simulations for the glueballino-initiated EAS's. Shower profiles and distributions of shower maxima are shown in Figs. 3–8 for three different initial energies, $E_0=10^{17}$, 10^{19}, and 10^{20} eV, for the glueballino as primary with different choices of the gluino mass. For comparison, the case of a primary proton is also shown. At the highest energy considered, $E_0=10^{20}$ eV,
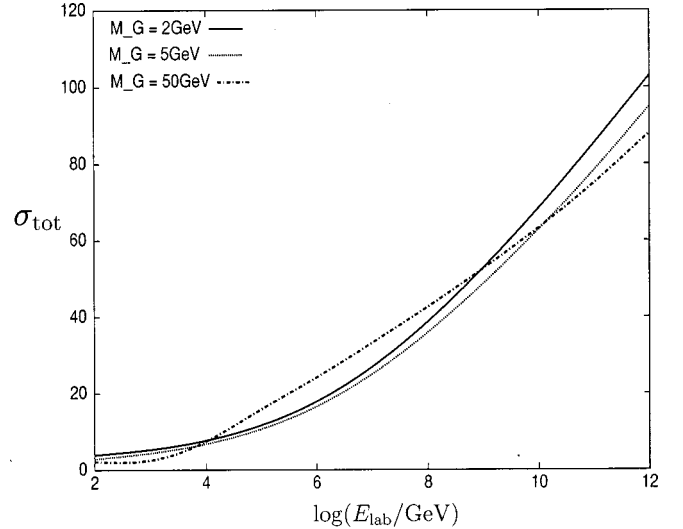

FIG. 1. Total glueballino-nucleon cross section σ_{tot} in mb as function of E_{lab} for $M_{\widetilde{G}}=2,5$, and 50 GeV.

the longitudinal shower profiles (Fig. 3) and the distribution of the shower maxima X_{max} (Fig. 4) of glueballino-induced EAS's are comparable with those induced by protons in the case of glueballino masses smaller than 5 GeV. As the glueballino mass increases, the shower develops deeper in the atmosphere with a less pronounced maximum. The fluctuations in X_{max} increase also for larger glueballino masses. The main reason for both effects is the competition between the large glueballino-nucleus cross section and the small inelasticity of the interactions: a heavy glueballino injects in one interaction only a small part of its energy into secondary hadronic and electromagnetic cascades, while interactions with a large momentum transfer are rare and only increase the fluctuations. Figure 4 clearly shows that the glueballino-induced EAS's drastically differ from the proton-induced showers for glueballino masses larger than 5 GeV, and hence
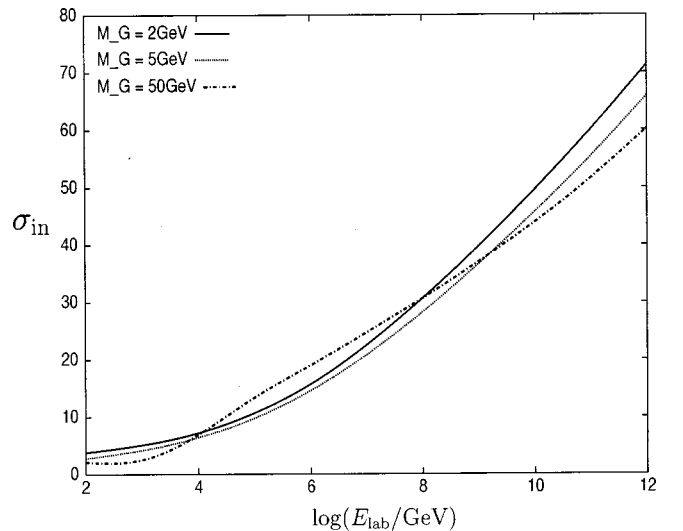

FIG. 2. Inelastic glueballino-nucleon cross section σ_{in} in mb as function of E_{lab} for $M_{\widetilde{G}}=2,5$, and 50 GeV.
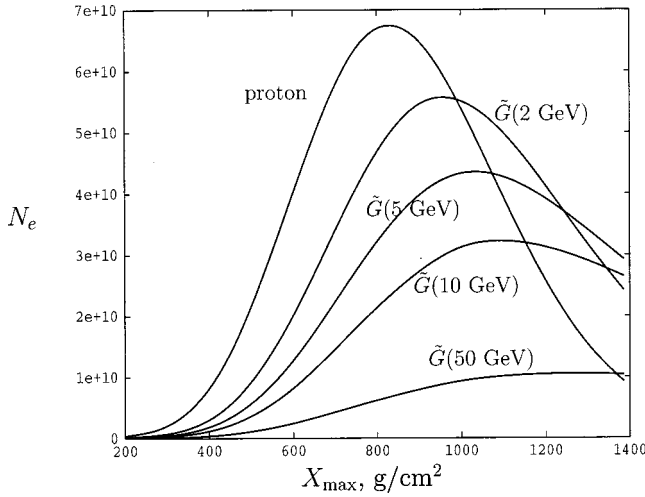
FIG. 3. Longitudinal shower profile for EAS's of energy $E_0 = 10^{20}$ eV initiated by protons and by glueballinos with $M_{\tilde{G}} = 2,5,10,$ and 50 GeV.

FIG. 5. Longitudinal shower profile for EAS's of energy $E_0 = 10^{19}$ eV initiated by protons and by glueballinos with $M_{\tilde{G}} = 2,5,10,$ and 50 GeV.

these showers can be distinguished even in the case of low statistics. In the case of a lighter glueballino with $M_{\tilde{G}} = 2$ GeV, more statistics is necessary to distinguish glueballino from proton, when only $X_{\max}$ measurements are used. The same conclusions can be drawn by comparing the shape of the calculated profiles for individual p- and $\tilde{G}$-induced EAS's of energy $E_0 = 3.2 \times 10^{20}$ eV with the corresponding measurements of the Fly's Eye Collaboration [58] (cf. Fig. 9). In doing so we choose only those showers that reach their maxima near the measured value $X_{\max} = 815 \pm 50$ g/cm². Then we average the profiles obtained and shift them to the same position of the shower maximum, $X_{\max} = 815$ g/cm². It is easy to see that for gluino masses larger than 5 GeV the shape of the calculated profile strongly disagrees with the experimental observations. Taking account of the Landau-Pomeranchuk-Migdal (LPM) effect results in only 5% reduction of the electron number in the shower maximum for proton-induced EAS's [29] and has an even smaller influence

on the $\tilde{G}$-induced showers due to the much softer π^0 spectrum in the glueballino interactions.

The calculated lateral distribution functions (LDF's) for electrons and muons ($E_\mu > 1$ GeV) at the AKENO observation level (900 g/cm²) are shown in Figs. 10 and 11 for the proton and glueballinos with masses 2 and 5 GeV (see also Tables III and IV). The plotted values are the LDF's of electrons and muons $\rho_e(R)$, $\rho_\mu(R)$ at different distances R from the shower core. Although these distributions are substantially different for showers initiated by glueballinos and protons, they can hardly be used to search for the light glueballino on the basis of existing data, e.g., of AGASA. An adequate tool for the glueballino search is the fluctuation of the muon density at distances $R \gtrsim 300$ m from the core. This method allows one in principle to discriminate showers initiated even by light glueballinos with $M_{\tilde{G}} \approx 2$ GeV from proton-initiated EAS's (see Table IV). With the currently accumulated statistics, ground-array experiments like AGASA
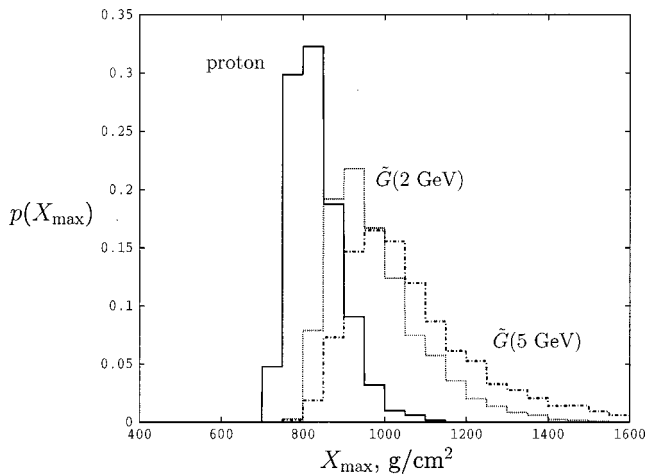

FIG. 4. Normalized distribution $p(X_{\max})$ of the shower maxima for EAS's of energy $E_0 = 10^{20}$ eV initiated by protons and by glueballinos with $M_{\tilde{G}} = 2$ and 5 GeV.
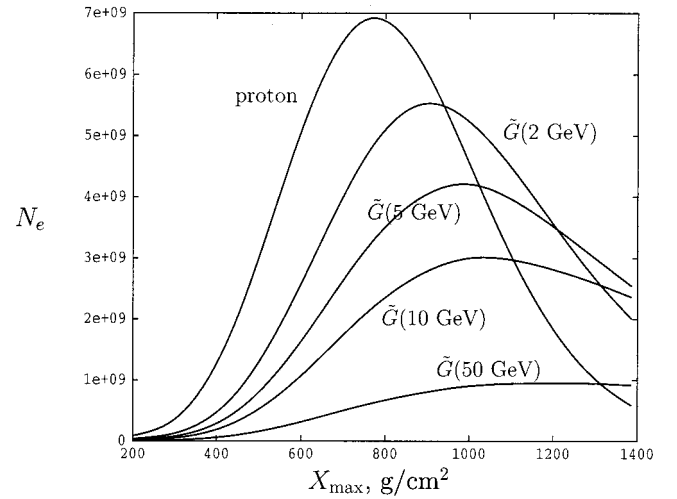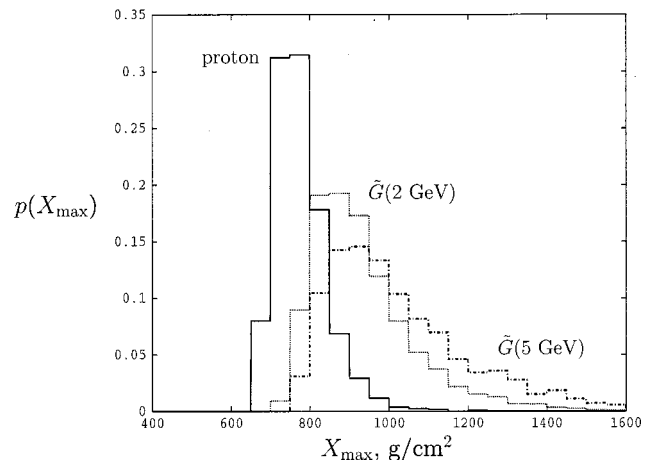

FIG. 6. Normalized distribution $p(X_{\max})$ of the shower maxima for EAS's of energy $E_0 = 10^{19}$ eV initiated by protons and by glueballinos with $M_{\tilde{g}} = 2$ and 5 GeV.
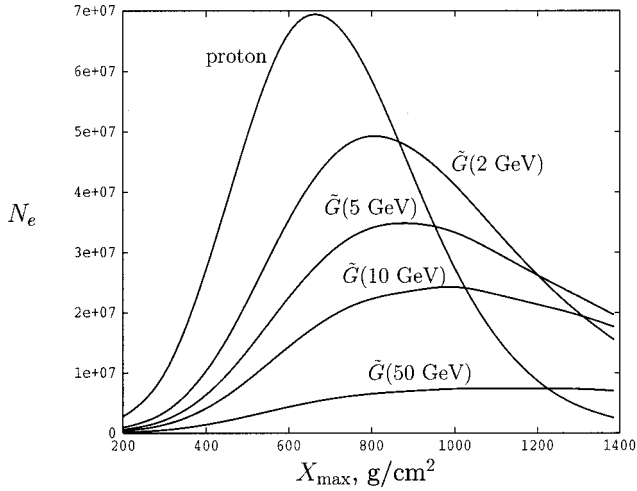
FIG. 7. Longitudinal shower profile for EAS's of energy $E_0 = 10^{17}$ eV initiated by protons and by glueballinos with $M_{\tilde{g}} = 2, 5, 10,$ and 50 GeV.

should be able to exclude a glueballino as light as 5 GeV as the main component of the UHECR's.

Finally, we shall compare our results with those of Albuquerque, Farrar, and Kolb (AFK) [48]. AFK have modified the event generator SIBYLL including the $\tilde{g}$ hadron ($\tilde{G}$) as a new particle. The interaction properties of the $\tilde{g}$ hadron were taken *ad hoc*. Two assumptions were used for the total cross section: $\sigma_{\text{tot}}(\tilde{G}p) \approx \sigma_{\text{tot}}(\pi p)$ (the favorite choice) and $\sigma_{\text{tot}}(\tilde{G}p) \approx 0.1\sigma_{\text{tot}}(\pi p)$. The mean energy fraction transferred from the $\tilde{G}$ hadron to the shower per interaction was modeled by a Peterson fragmentation function. Hard interactions with the production of minijets by the incident $\tilde{G}$ hadron were neglected.

It is easy to see that these modifications are not self-consistent. Indeed, on one hand the authors assume a large $\tilde{G}p$ cross section, while on the other hand they neglect the hard processes (production of minijets), which give the
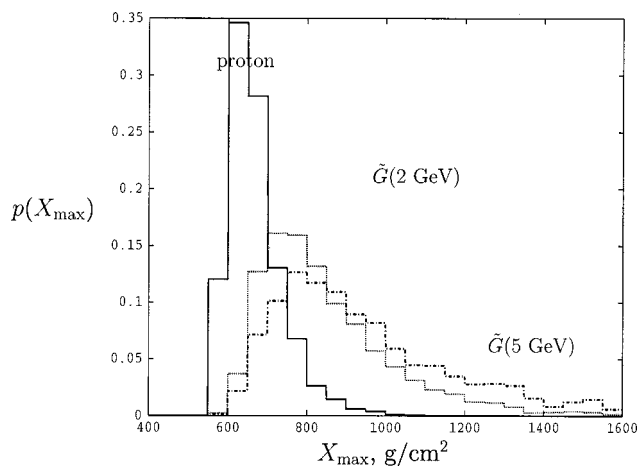
dominant contribution to the $\tilde{G}p$ cross section and make it large. In fact, our calculations explicitly show that at ultra-high energies the $\tilde{G}p$ cross section and particle production are dominated by hard interactions for both light and heavy gluinos. For light gluinos, valence gluons and sea partons have enough momenta for hard interactions. For heavy gluinos, their own "(direct)" hard interaction dominates. Soft interactions without the production of parton jets are negligible in both cases.

To elucidate the reason for the failure of the AFK approach, we have calculated the total $\tilde{G}$ nucleon cross section switching off the hard interaction (see the fifth entry σ_{AFK} in Tables I and II): At energies relevant for UHECR's, the in-
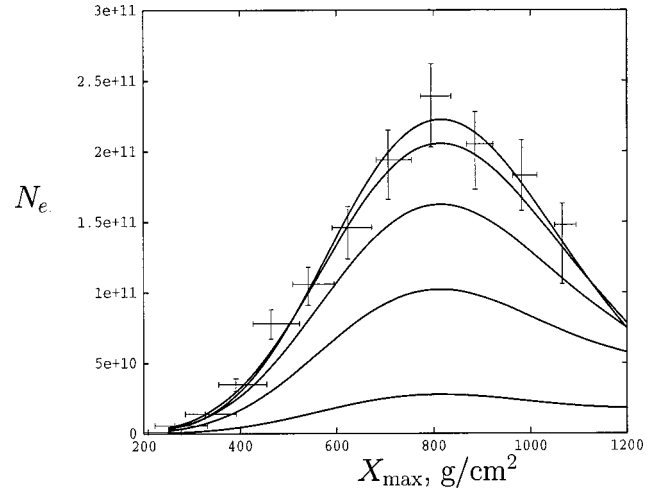

FIG. 9. Comparison of Flye's Eye highest-energy event with the longitudinal shower profile for EAS's of energy $E_0 = 3 \times 10^{20}$ eV initiated (from top to bottom) by protons and by glueballinos with $M_{\tilde{g}} = 2, 5, 10,$ and 50 GeV. The shower profiles are shifted so that their $X_{\max}$ agrees with the observed shower maximum.

FIG. 8. Normalized distribution $p(X_{\max})$ of the shower maxima for EAS's of energy $E_0 = 10^{17}$ eV initiated by protons and by glueballinos with $M_{\tilde{g}} = 2$ and 5 GeV.
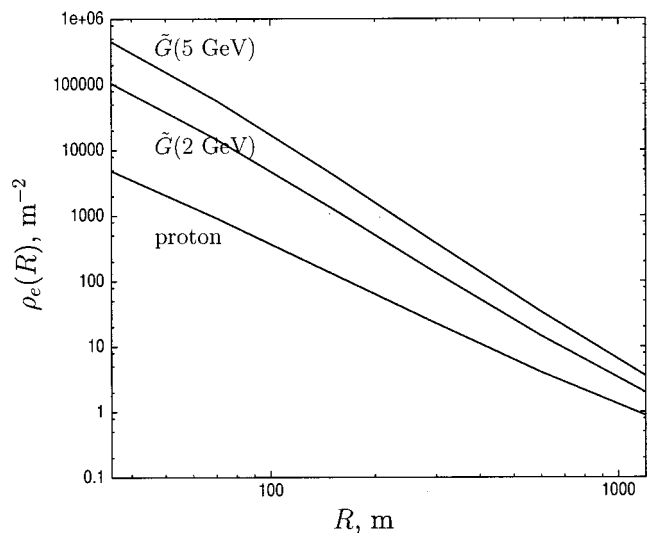

FIG. 10. Electron LDF $\rho_e(R)$ in m^{-2} at the AKENO observation level as function of the distance R (in m) from the shower core for EAS's of energy $E_0 = 10^{20}$ eV initiated by protons and by glueballinos with $M_{\tilde{g}} = 2$ and 5 GeV.

FIG. 11. Muon LDF $(E_\mu > 1 \text{ GeV})\rho_\mu(R)$ in m^{-2} at the AKENO observation level as function of the distance R (in m) from the shower core for EAS's of energy $E_0 = 10^{20}$ eV initiated by protons and by glueballinos with $M_{\tilde{g}} = 2$ and 5 GeV.
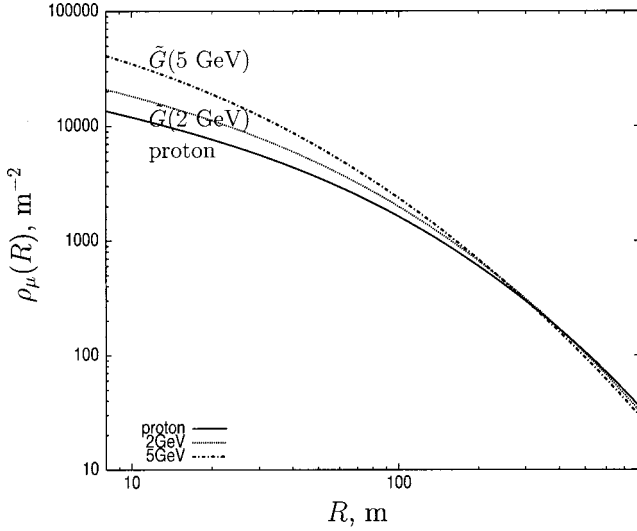
teractions considered by AFK are only subdominant and result in much smaller total cross sections compared with ours or those assumed by AFK.

IV. ENERGY LOSSES OF GLUEBALLINOS ON CMBR PHOTONS AND GLUEBALLINO ENERGY SPECTRUM

Although both valence constituents of the glueballino are electrically neutral, UHE glueballinos lose energy due to scattering on CMBR photons. The value of the cutoff in its energy spectrum is determined by the transition from adiabatic energy losses (redshift) to rapidly increasing energy losses due to the reaction $\tilde{G} + \gamma \rightarrow \tilde{G} + \pi^0$ at higher energies. This process cannot occur due to π^0 exchange in the t channel. The dominant contribution is given by the resonant formation of $\tilde{g}\bar{q}q$ states in the s channel. The mass spectrum of $\tilde{g}\bar{q}q$ states was calculated as a function of the gluino mass in Ref. [59] in the MIT bag model. The lowest $\tilde{g}\bar{q}q$ state found was the spin-1/2 state $\tilde{\rho}_{1/2}$; its mass difference from the glueballino, however, except for $m_{\tilde{G}} < 1.2$ GeV, is too small as to allow the decay $\tilde{\rho}_{1/2} \rightarrow \tilde{G} + \pi^0$, cf. Table V. We assume

TABLE III. Normalized 1σ fluctuations of the electron LDF $\sigma_{\rho_e(R)}/\rho_e(R)$ at the AKENO observation level for EAS's of energy $E_0 = 10^{20}$ eV initiated by protons and glueballinos of masses 2, 5, and 10 GeV.

	R (m)						
	10	50	100	200	300	600	1200
Proton	0.077	0.054	0.068	0.095	0.11	0.15	0.18
$\tilde{G}$(2 GeV)	0.20	0.25	0.27	0.30	0.31	0.34	0.36
$\tilde{G}$(5 GeV)	0.33	0.37	0.39	0.41	0.43	0.45	0.47
$\tilde{G}$(10 GeV)	0.40	0.43	0.45	0.47	0.48	0.50	0.52

TABLE IV. Normalized 1σ fluctuations of the muon LDF ($E_\mu > 1$ GeV) $\sigma_{\rho_\mu(R)}/\rho_\mu(R)$ at the AKENO observation level for EAS of energy $E_0 = 10^{20}$ eV initiated by protons and glueballinos of masses 2, 5 and 10 GeV.

	R (m)					
	10	100	200	300	600	1200
Proton	0.19	0.16	0.16	0.17	0.20	0.25
$\tilde{G}$(2 GeV)	0.18	0.20	0.24	0.27	0.33	0.41
$\tilde{G}$(5 GeV)	0.23	0.30	0.34	0.37	0.43	0.51
$\tilde{G}$(10 GeV)	0.30	0.36	0.40	0.42	0.48	0.55

therefore that the first resonance in the s channel is an excited $\tilde{\rho}_{1/2}^*$ state; for its mass $m(\tilde{\rho}_{1/2}^*)$ we use $m(\tilde{\rho}_{1/2}^*) = m(\tilde{\rho}_{1/2}) + 730$ MeV, guided by the mass difference between the $\rho(770)$ and the $\rho(1400)$. The Breit-Wigner cross section for the reaction $\tilde{G} + \gamma \rightarrow \tilde{\rho}_{1/2} \rightarrow \tilde{G} + \pi^0$ is [42]

$$\sigma(s) = \frac{2\pi}{p_{\text{c.m.}}^2} \frac{B_{\text{in}}B_{\text{out}}\Gamma_{\text{tot}}^2 m_{\tilde{\rho}}^2}{(s - m_{\tilde{\rho}}^2)^2 + (m_{\tilde{\rho}}\Gamma_{\text{tot}})^2}, \quad (17)$$

where $p_{\text{c.m.}}$ and $\sqrt{s}$ are the momentum and the total energy of the particles in the c.m. system, $m_{\tilde{\rho}}$ is the mass of the $\tilde{\rho}_{1/2}/\tilde{\rho}_{1/2}^*$ particle, and Γ_{tot} is its total decay width. Finally, B_{in} and B_{out} denote the branching ratios of the resonance to the initial and final states.

For the determination of the unknown branching ratios B_{in}, B_{out}, and the total decay rate Γ_{tot}, we can use the analogy between the glueballino and the pion together with scaling arguments as in Sec. II B for both the $\tilde{\rho}_{1/2}$ and the $\tilde{\rho}_{1/2}^*$. Then

$$B_{\text{out}} = \Gamma(\tilde{\rho}_{1/2} \rightarrow \tilde{G} + \pi^0)/\Gamma_{\text{tot}}(\tilde{\rho}_{1/2}) \simeq 1 \quad (18)$$

and

$$B_{\text{in}} = \frac{\Gamma(\tilde{\rho}_{1/2} \rightarrow \tilde{G} + \gamma)}{\Gamma_{\text{tot}}(\tilde{\rho}_{1/2})} \simeq \frac{\Gamma(\rho^0 \rightarrow \pi^0 + \gamma)}{\Gamma_{\text{tot}}(\rho)} \simeq 7 \times 10^{-4}. \quad (19)$$

The total decay rate $\Gamma_{\text{tot}}(\tilde{\rho}_{1/2}) \propto g_{\tilde{\rho}}^2 m_{\tilde{\rho}}$ can be calculated using $m_{\tilde{\rho}}$ from Ref. [59] together with

$$g_{\tilde{\rho}} = \frac{m_\rho}{m_{\tilde{\rho}}} g_\rho. \quad (20)$$

TABLE V. The masses of the glueballino $\tilde{G}$ and the $\tilde{\rho}_{1/2}$ as functions of the gluino mass $m_{\tilde{g}}$ according to Ref. [59].

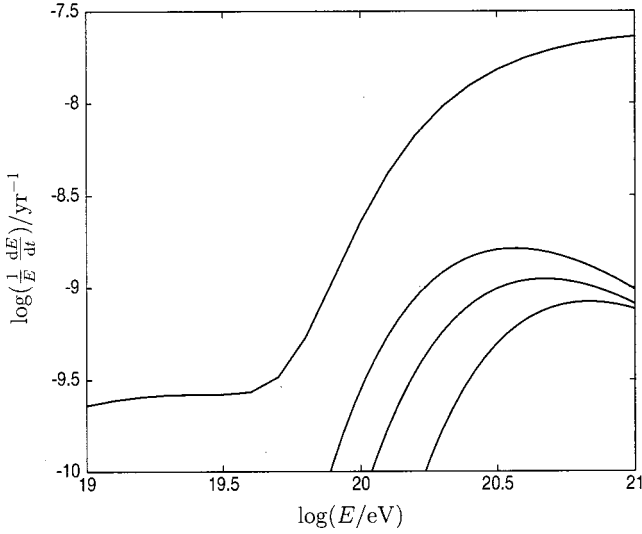| $m_{\tilde{g}}/$(GeV)	0.64	1.04	1.48	2.41
$M_{\tilde{G}}/$(GeV)	1.00	1.50	2.00	3.00
$m_{\tilde{\rho}_{1/2}}/$(GeV)	1.17	1.58	2.04	3.03

FIG. 12. Energy losses $(1/E)(dE\,dt)$ yr^{-1} of protons and of glueballinos with $M_{\tilde{g}}=1.5$, 2, and 3 GeV (from top to bottom) due to scattering on the CMBR as function of their laboratory energy E(eV).

The maximum of the photo-pion production cross section for the glueballino is at least a factor of 8 smaller than for the proton due to the differences in B_{in}, the spin factors, and $p_{c.m.}$. We neglect multipion production $\tilde{G}+\gamma\rightarrow\tilde{G}+\pi^{+}+\pi^{-}$, which operates at energies above those we are interested in. The nonresonant contributions have been calculated in the vector dominance model and give only a small contribution to the total cross section of the glueballino. The hard processes with gluon exchange are important only at high energies.

The energy loss of a particle scattering on CMBR photons is given by [60]

$$-\frac{1}{E}\frac{dE}{dt}=\frac{T}{2\pi^2\Gamma^2}\int_{E_{th}}^{\infty}dE_r\,\sigma(E_r)y(E_r)E_r$$

$$\times\left\{-\ln\left[1-\exp\left(-\frac{E_r}{2\Gamma T}\right)\right]\right\}. \quad (21)$$

Here, Γ is the Lorentz factor of the particle in the CMBR frame, E_r is the energy of a CMBR photon in the rest system of the glueballino, $E_{th}=m_\pi(1+m_\pi/2m_{\tilde{G}})$ is the threshold energy in the glueballino rest system, and y is the average fraction of energy lost by the glueballino in a collision, which for one-pion production is

$$y(E_r)=\frac{E_r}{m_{\tilde{G}}}\frac{1+m_\pi^2/2E_r m_{\tilde{G}}}{1+2E_r/m_{\tilde{G}}}. \quad (22)$$

In Fig. 12, we show the energy losses of a glueballino with mass $M_{\tilde{g}}=1.5$, 2, and 3 GeV compared to the losses of a proton (from [18]).

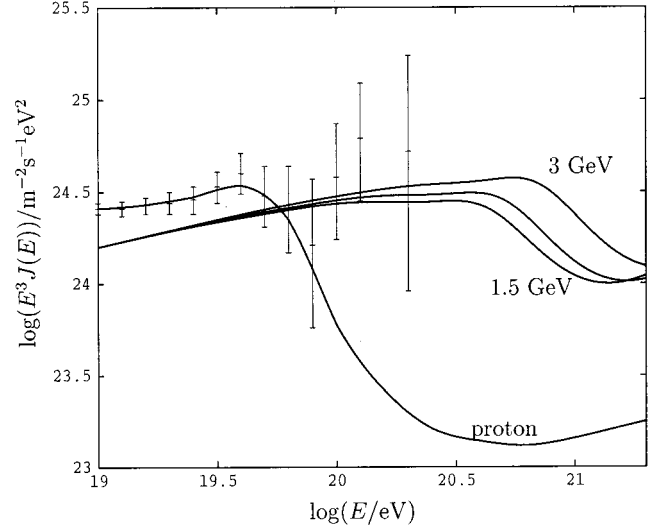The energy spectrum dN/dE of glueballinos emitted by diffuse sources is at the present redshift $z=0$ given by

FIG. 13. Diffuse glueballino flux from uniformly distributed sources with injection spectra $dN/dE\propto E^{-2.7}$ for $M_{\tilde{G}}=1.5$, 2, and 3 GeV, compared with proton flux and observational data from AGASA. Either the gluino flux or a combination of proton and gluino fluxes can fit the data.

$$\frac{dN}{dE}(0)=a\int_0^{z_{max}}dz_g(1+z_g)^{-5/2}\frac{dN}{dE_g}(z_g)\frac{dE_g(E,z_g)}{dE},$$
$$(23)$$

where $dN/dE_g(t_g)$ is the injection spectrum at redshift z_g and a is a constant depending mainly on the source emissivity. We calculated $dE_g(E,z_g)/dE$ as described in Ref. [61]. For the injection spectrum we used $dN/dE_g(z_g)\sim E_g^{-2.7}$ with a maximal redshift $z_{max}=2$, both without an intrinsic energy cutoff (Fig. 13) and with a cutoff at $E=1\times10^{22}$ eV (Fig. 14).
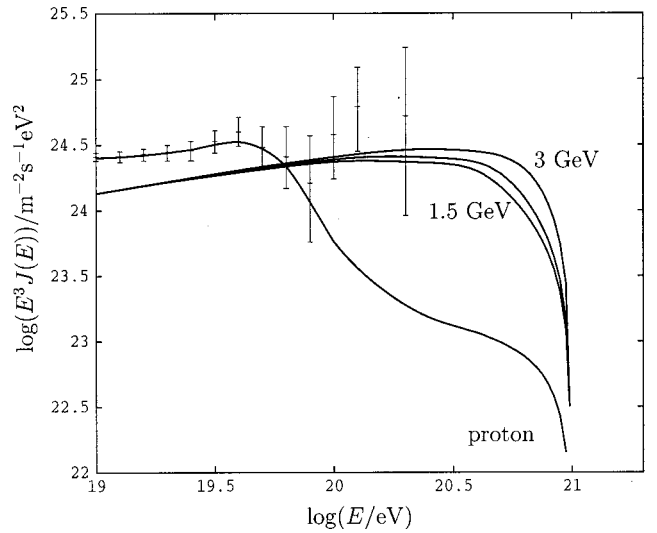

FIG. 14. Diffuse glueballino flux from uniformly distributed sources with injection spectra $dN/dE\propto E^{-2.7}$ and intrinsic cutoff $E=10^{21}$ eV for $M_{\tilde{G}}=1.5$, 2, and 3 GeV, compared with proton flux and observational data from AGASA. Either the gluino flux or a combination of proton and gluino fluxes can fit the data.

TABLE VI. The upper 90% C.L. limit on the invariant cross sections $Ed^3\sigma/d^3p$ (second line) for measured masses M_{meas} (first line) given by the Gustafson experiment. The fourth line gives the calculated invariant cross sections for gluino production in pp interaction at $E_{p,\text{lab}}=300$ GeV and for gluino mass $m_{\widetilde{G}}$ (third line). All cross sections are in cm^2/GeV^2.

M_{meas} GeV	2	3	4	6	8	10
90% C. L.	1.0×10^{-32}	3.6×10^{-33}	1.3×10^{-33}	5.3×10^{-33}	2.0×10^{-33}	1.7×10^{-33}
$m_{\widetilde{G}}$ (GeV)	2	3	4	6	8	10
$Ed^3\sigma/d^3p$	3.8×10^{-30}	1.7×10^{-31}	1.1×10^{-32}	4.2×10^{-35}	3.9×10^{-38}	8.9×10^{-43}

The calculated diffuse spectra are presented for three different masses of the glueballino, $m_{\widetilde{G}}=1.5$, 2, and 3 GeV, and for comparison the corresponding proton spectra are also shown. The cutoff in the glueballino spectra is shifted to larger energies not only because of $m_{\widetilde{G}}>m_N$ but also because of the large mass gap between $\widetilde{G}$ and $\widetilde{\rho}^*_{1/2}$. Moreover, the smaller cross section and energy transfer make the cutoff less pronounced. The calculated spectra for all three masses are in agreement with the observations [46]. However, the observed flux above the GZK cutoff can be reproduced only if either the glueballino injection spectrum is rather flat or if at energies $E\sim10^{19}$ eV also glueballinos are a non-negligible component of the cosmic ray flux. Finally, we stress that the exact form of the glueballino energy spectrum depend rather strongly on the mass spectrum of the hadronic bound states of the gluino; still our general observations (shift of the cutoff to larger energies, less pronounced cutoff) are independent of the details of the mass spectrum.

V. EXPERIMENTAL LIMITS FROM BEAM-DUMP EXPERIMENTS

The experiment Fermilab E-0330 by Gustafson *et al.* was designed to search for neutral hadrons with masses $\gtrsim2$ GeV and lifetimes $\gtrsim10^{-7}$ s [47]. In contrast to the recent experiments [35–38], the Gustafson experiment was sensitive to long-lived or stable hadrons. It set upper limits on the production cross section of these hadrons in the mass range 2–12 GeV which are given in the second line of Table VI. However, the relation between the measured mass M_{meas} in the Gustafson experiment and the physical mass of $\widetilde{G}$ hadrons needs careful consideration.

In the Gustafson experiment, short pulses of protons with energy 300 GeV produced in the beam-dump target neutral secondary particles, which were detected in a calorimeter at distance $l=590$ m from the target. The calorimeter had the total thickness $X_{\text{cal}}=900$ g/cm^2, and it was assumed that a particle loses all its energy therein. Then the measured difference in the time of flight δt of massive secondaries and photons determines the mass of the secondary,

$$M_{\text{meas}}=(2cE^2_{\text{loss}}\delta t/l)^{1/2}. \qquad (24)$$

Here, the energy loss E_{loss} in the calorimeter is taken as the energy of a particle. In fact, however, a $\widetilde{g}$ hadron loses only a part of its energy in the calorimeter: E_{loss}/E

$=K_{\text{inel}}X_{\text{cal}}/X_{\text{int}}$, where X_{int} is the inelastic interaction length. Then the physical mass $M_{\widetilde{G}}$ of a $\widetilde{g}$ hadron is connected to the measured mass as

$$M_{\text{meas}}=(E_{\text{loss}}/E)M_{\widetilde{G}}. \qquad (25)$$

In the case of a glueballino, one obtains from Eq. (25) together with the data of Table I $M_{\text{meas}}\sim1$ GeV for $M_{\widetilde{G}}=2$ and 5 GeV. Thus, in both cases glueballinos fall in the region of neutron background and therefore these masses are allowed.

Are heavier masses of $\widetilde{g}$ hadrons allowed by the Gustafson experiment?

We have calculated the cross section for gluino production in pp collision via the two subprocesses $gg\rightarrow\widetilde{g}\widetilde{g}$ and $q\bar{q}\rightarrow\widetilde{g}\widetilde{g}$ at next-to-leading order [62] for $E_{\text{lab}}=300$ GeV using the program PROSPERO [63]. As parton distributions we have chosen those of Glück, Reya, and Vogt [64], while we have used $Q=m_{\widetilde{g}}$ as renormalization and factorization scales. In Table VI, the production cross sections averaged over the region allowed by the experimental cuts are compared with the upper limits from the Gustafson experiment. Inspection of Table VI for larger masses shows that the calculated cross sections are smaller than the upper limits given in the second line. We conclude that the results of the Gustafson experiment do not exclude $\widetilde{g}$ hadrons.

A modified Gustafson experiment has great potential to discover light $\widetilde{g}$ hadrons in the window 2–4 GeV or to reliably exclude them. For this aim, a thicker calorimeter is needed. If $\widetilde{g}$ hadrons lose all their energy in the calorimeter, then $M_{\text{meas}}\approx M_{\widetilde{G}}$, and the third and fourth lines of Table VI show that the calculated cross sections for $M_{\widetilde{G}}$ in the interval 2–4 GeV are larger than the experimental upper bounds. This means that the $\widetilde{g}$ hadron in this mass window can be discovered or excluded, if the calorimeter is thick enough. Taking into account the large penetrating power of $\widetilde{g}$ hadrons the neutron background can be greatly reduced by placing the absorber behind a target whose thickness is tuned to absorb the neutrons but to be transparent for $\widetilde{g}$ hadrons.

The signature of $\widetilde{g}$ hadrons is given by the compatibility of the gluino production cross section with the measured flux of detected particles. The path length and the average fraction of lost energy will serve as further indicators. The measured properties of $\widetilde{g}$ hadrons will then allow reliable calcu-

lations of $\tilde{g}$-hadron production in astrophysical sources and their detection in EAS's.

VI. CONCLUSIONS

There are two mass windows where a light gluino is marginally allowed: $m_{\tilde{g}} \lesssim 3$ GeV and $25 \lesssim m_{\tilde{g}} \lesssim 35$ GeV. The first window is disfavored by the gluino contribution to the running of α_s and to the color coefficients. The lightest $\tilde{g}$ hadron is heavier than the gluino by the mass of the constituent gluon or quarks. The existence of a light *quasistable* $\tilde{g}$ hadron, corresponding to the first window for gluino masses, crucially depends on whether the neutral or charged $\tilde{g}$ hadron is the lightest one. A light quasistable charged $\tilde{g}$ hadron is forbidden by the production of "wild hydrogen" in the earth's atmosphere by cosmic rays. The case that the lightest $\tilde{g}$ hadron is neutral is also forbidden, if it forms a bound state with the proton ("wild deuteron"). The status of the light gluino and lightest $\tilde{g}$ hadron can be clarified by further theoretical analysis. At present we conservatively consider the first gluino window as disfavored, but not excluded.

As the carrier of the UHE signal, the light $\tilde{g}$ hadrons with a mass larger than 1.5 GeV have a spectrum with the GZK cutoff beyond the observed energy range (see Fig. 13). Together with accelerator limits on the gluino mass, $m_{\tilde{g}} < 3$ GeV, this leaves for $\tilde{g}$ hadron masses the narrow window 1.5–4 GeV. The other window allowed by accelerator experiments is 25–35 GeV.

In this paper we have studied the interaction of $\tilde{g}$ hadrons with nucleons and nuclei and the development of UHE EAS's initiated by such particles. In practice, we have considered the special case of a glueballino as the primary particle. We think, however, that any other $\tilde{g}$ hadron with equal mass has essentially the same interaction properties. We have calculated the glueballino-nucleon inelastic and total cross sections for different masses of glueballinos (see Figs. 1 and 2). The longitudinal development of the EAS with energy 3×10^{20} eV in the atmosphere is shown in Fig. 9. One can see that glueballinos heavier than 5 GeV resemble penetrating particles. The profiles shown in the figure were directly measured in the Fly's Eye experiment, and the data are quite different from the graphs displayed here for heavy glueballinos. The second mass window 25–35 GeV can already be reliably excluded on the basis of these measurements, although a detailed analysis is desirable.

The showers produced by $\tilde{g}$ hadrons from the low-mass window are similar to proton-initiated showers in all characteristics (see the longitudinal profiles in Figs. 3, 5, and 7, the distributions over $X_{\max}$ in Figs. 4, 6, and 8, the lateral distributions for electrons and muons in Figs. 10 and 11, and the fluctuations in muon and electron densities in Tables III and IV). In principle, the best possibility to distinguish the showers produced by $\tilde{g}$ hadrons with mass 2 GeV from the proton-induced showers is the fluctuations in the muon density at large distances $d > 600$ m (see Table III). However, the statistics of the largest array at present, AGASA, is not sufficient for such a discrimination. The large $X_{\max}$ tail in the distribution of showers initiated by $\tilde{g}$ hadrons over $X_{\max}$ offers for HiRes or AUGER another, more promising possibility to (dis) prove light gluinos as UHE primaries.

More reliably, the quasistable 2–3 GeV $\tilde{g}$ hadron could be found in a specially designed accelerator beam-dump experiment (see Sec. V). In this experiment, it would be possible to discover supersymmetry (light gluino) and to find a new primary for the UHE cosmic signal.

ACKNOWLEDGMENTS

[1] G. Auriemma, L. Maiani, and S. Petrarca, Phys. Lett. **164B**, 179 (1985).

[2] V.S. Berezinskii and B.L. Ioffe, Sov. Phys. JETP **63**, 920 (1986); ITEP, Report No. 127, 1985.

[3] D.J. Chung, G.R. Farrar, and E.W. Kolb, Phys. Rev. D **57**, 4606 (1998).

[4] G.R. Farrar and P.L. Biermann, Phys. Rev. Lett. **81**, 3579 (1998).

[5] For recent reviews, see A.V. Olinto, Phys. Rep. **333**, 329 (2000); M. Nagano and A.A. Watson, Rev. Mod. Phys. **72**, 689 (2000); P. Bhattacharjee and G. Sigl, Phys. Rep. **327**, 110 (2000); V. Berezinsky, Nucl. Phys. B (Proc. Suppl.) **70**, 419 (1999); S. Yoshida and H. Dai, J. Phys. G **24**, 905 (1998).

[6] S.I. Dubovsky, P.G. Tinyakov, and I.I. Tkachev, Phys. Rev. Lett. **85**, 1154 (2000); Z. Fodor and S.D. Katz, Phys. Rev. D **63**, 023002 (2000).

[7] K. Greisen, Phys. Rev. Lett. **16**, 748 (1966); G.T. Zatsepin and V.A. Kuzmin, JETP Lett. **4**, 78 (1966).

[8] V. Berezinsky and G.T. Zatsepin, Sov. J. Nucl. Phys. **13**, 11 (1971); V. Berezinsky, S.I. Grigorieva, and G.T. Zatsepin, in Proceedings of the 14th International Cosmic Ray Conference, Munich, 1975, Vol. 2, p. 711.

[9] L.N. Epele and E. Roulet, J. High Energy Phys. **10**, 009 (1998).

[10] V. Berezinsky, Sov. J. Nucl. Phys. **11**, 222 (1970); R. Protheroe and P. Biermann, Astropart. Phys. **6**, 45 (1996).

[11] N. Hayashida *et al.*, Phys. Rev. Lett. **73**, 3491 (1994).

[12] D. Bird *et al.*, Astrophys. J. **441**, 144 (1995).

[13] AGASA Collaboration, N. Sakaki, in Proceedings of the 27th International Cosmic Ray Conference, Hamburg, 2001, p. 333.

[14] J.N. Bahcall and E. Waxman, Astrophys. J. **542**, 542 (2000).

[15] M. Blanton, P. Blasi, and A.V. Olinto, Astropart. Phys. **15**, 275 (2001).

[16] R.D. Blandford, Phys. Scr. **T85**, 191 (2000).

[17] S.T. Sculli and F.W. Stecker, Astropart. Phys. **14**, 207 (2000).

[18] V. Berezinsky, A.Z. Gazizov, and S.I. Grigorieva, hep-ph/0107306.

[19] V. Berezinsky, M. Kachelrieß, and A. Vilenkin, Phys. Rev.

Lett. **79**, 4302 (1997); V.A. Kuzmin and V.A. Rubakov, Phys. At. Nucl. **61**, 1028 (1998).

[20] C.T. Hill, D.N. Schramm, and T.P. Walker, Phys. Rev. D **36**, 1007 (1987).

[21] T.J. Weiler, Astropart. Phys. **11**, 303 (1999); D. Fargion, B. Mele, and A. Salis, Astrophys. J. **517**, 725 (1999); G. Gelmini and A. Kusenko, Phys. Rev. Lett. **82**, 5202 (1999); **84**, 1378 (2000).

[22] V.S. Berezinsky and G.T. Zatsepin, Phys. Lett. **28B**, 423 (1969); G. Domokos and S. Nussinov, Phys. Lett. B **187**, 372 (1987); J. Bordes, H. Chan, J. Faridani, J. Pfaudler, and S.T. Tsou, Astropart. Phys. **8**, 135 (1998); G. Domokos and S. Kovesi-Domokos, Phys. Rev. Lett. **82**, 1366 (1999); P. Jain, D.W. McKay, S. Panda, and J.P. Ralston, Phys. Lett. B **484**, 267 (2000); but see also G. Burdman, F. Halzen, and R. Gandhi, *ibid.* **417**, 107 (1998); M. Kachelrieß and M. Plümacher, *ibid.* **62**, 103006 (2000).

[23] T.W. Kephart and T.J. Weiler, Astropart. Phys. **4**, 271 (1996); S. Bonazzola and P. Peter, *ibid.* **7**, 161 (1997).

[24] L. Gonzales-Mestres, Nucl. Phys. B (Proc. Suppl.) **48**, 131 (1996); S. Coleman and S.L. Glashow, Phys. Rev. D **59**, 116008 (1999); R. Aloisio, P. Blasi, P. Ghia, and A. Grillo, *ibid.* **62**, 053010 (2000).

[25] G. Sigl, D.F. Torres, L.A. Anchordoqui, and G.E. Romero, Phys. Rev. D **63**, 081302 (2001); A. Virmani, S. Bhattacharya, P. Jain, S. Razzaque, J.P. Ralston, and D.W. McKay, astro-ph/0010235; L.A. Anchordoqui *et al.*, Mod. Phys. Lett. A **16**, 2033 (2001).

[26] P.G. Tinyakov and I.I. Tkachev, JETP Lett. **74**, 499 (2001); astro-ph/0102476.

[27] V. Berezinsky and M. Kachelrieß, Phys. Lett. B **422**, 163 (1998).

[28] F. Halzen, R.A. Vazquez, T. Stanev, and H.P. Vankov, Astropart. Phys. **3**, 151 (1995).

[29] N.N. Kalmykov, S.S. Ostapchenko, and A.I. Pavlov, Phys. At. Nucl. **58**, 1728 (1995).

[30] G.R. Farrar, Phys. Rev. Lett. **76**, 4111 (1996).

[31] S. Raby, Phys. Lett. B **422**, 158 (1998).

[32] S. Raby and K. Tobe, Nucl. Phys. **B539**, 3 (1999).

[33] M.B. Voloshin and L.B. Okun, Sov. J. Nucl. Phys. **43**, 495 (1986).

[34] F. Buccella, G.R. Farrar, and A. Pugliese, Phys. Lett. **153B**, 311 (1985).

[35] KTeV Collaboration, J. Adams *et al.*, Phys. Rev. Lett. **79**, 4083 (1997).

[36] NA48 Collaboration, V. Fanti *et al.*, Phys. Lett. B **446**, 117 (1999).

[37] KTeV Collaboration, A. Alavi-Harati *et al.*, Phys. Rev. Lett. **83**, 2128 (1999).

[38] E761 Collaboration, I.F. Albuquerque *et al.*, Phys. Rev. Lett. **78**, 3252 (1997).

[39] F. Csikor and Z. Fodor, Phys. Rev. Lett. **78**, 4335 (1997).

[40] ALEPH Collaboration, R. Barate *et al.*, Z. Phys. C **76**, 1 (1997).

[41] G.R. Farrar, Nucl. Phys. B (Proc. Suppl.) **62**, 485 (1998).

[42] Particle Data Group, C. Caso *et al.*, Eur. Phys. J. C **3**, 1 (1998).

[43] H. Baer, K. Cheung, and J.F. Gunion, Phys. Rev. D **59**, 075002 (1999).

[44] A. Mafi and S. Raby, Phys. Rev. D **62**, 035003 (2000).

[45] R.N. Mohapatra and S. Nussinov, Phys. Rev. D **57**, 1940 (1998).

[46] M. Takeda *et al.*, Phys. Rev. Lett. **81**, 1163 (1998).

[47] H.R. Gustafson *et al.*, Phys. Rev. Lett. **37**, 474 (1976).

[48] I.F. Albuquerque, G.R. Farrar, and E.W. Kolb, Phys. Rev. D **59**, 015021 (1999).

[49] N.N. Kalmykov, S.S. Ostapchenko, and A.I. Pavlov, Nucl. Phys. B (Proc. Suppl.) **52B**, 17 (1997); N.N. Kalmykov and S.S. Ostapchenko, Report No. INP MSU 98-36/537, Moscow, 1998.

[50] N.N. Kalmykov, S.S. Ostapchenko, and A.I. Pavlov, Izv. Ross. Akad. Nauk, Ser. Fiz. **58**, 21 (1994) [Bull. Russ. Acad. Sci (USA), Phys. Ser. **58**, 1966 (1994)].

[51] J. Hoerandel, in Proceedings of the 26th International Salt Lake City, Cosmic Ray Conference, 1999, Vol. 1, p. 131.

[52] A.B. Kaidalov and K.A. Ter-Martirosyan, Phys. Lett. **117B**, 247 (1982).

[53] R.J. Glauber, in *Lectures in Theoretical Physics*, edited by W.E. Britten (Inter-Science, New York, 1959).

[54] V.N. Gribov, Zh. Eksp. Teor. Fiz. **59**, 892 (1969) (in Russian).

[55] N.N. Kalmykov and S.S. Ostapchenko, Phys. At. Nucl. **56**, 346 (1993).

[56] S. Ostapchenko, T. Thouw, and K. Werner, Nucl. Phys. B (Proc. Suppl.) **52**, 3 (1997).

[57] G. Marchesini and B.R. Webber, Nucl. Phys. **B238**, 1 (1984).

[58] D.J. Bird *et al.*, Astrophys. J. **441**, 144 (1995).

[59] M. Chanowitz and S. Sharpe, Phys. Lett. **126B**, 227 (1983). We use the values given in their Table 2 for $C_{TE}=1$.

[60] V.S. Berezinsky, S.V. Bulanov, V.L. Ginzburg, V.A. Dogiel, and V.S. Ptuskin, *Astrophysics of Cosmic Rays* (Elsevier, Amsterdam, 1990), Chap. 4.

[61] V.S. Berezinsky and S.I. Grigorieva, Astron. Astrophys. **199**, 1 (1988).

[62] W. Beenakker, R. Höpker, M. Spira, and P.M. Zerwas, Nucl. Phys. **B492**, 51 (1997).

[63] W. Beenakker, R. Höpker, and M. Spira, hep-ph/9611232.

[64] M. Glück, E. Reya, and A. Vogt, Z. Phys. C **67**, 433 (1995).